

Supporting information

A novel tripeptide model of nickel superoxide dismutase

Mary E. Krause[†], Amanda M. Glass[†], Timothy A. Jackson[†], and Jennifer S. Laurence^{*‡}

[†]*Department of Chemistry, University of Kansas, Lawrence, KS 66045*

[‡]*Department of Pharmaceutical Chemistry, University of Kansas, Lawrence, KS 66045*

*e-mail: laurencj@ku.edu

Experimental Details.

Figure S1. ESI-MS of Ni-NCC in 50 mM borate, pH 9.3.

Figure S2. CD data from pH titration of Ni-NCC in 50 mM borate.

Figure S3. MCD spectra at 7T of Ni-NCC at pH 10 in borate buffer/sucrose solution.

Figure S4. Room temperature and low temperature CD spectra of Ni-NCC.

Figure S5. Energies and models of possible structures of Ni-NCC.

Figure S6. CV of Ni-NCC.

Figure S7. CD and absorption spectra of Ni-NCC, Ni-GGGCC, and Ni-GGNCC.

Table S1. Deconvolution of peaks in absorption and CD spectra of Ni-NCC.

Experimental:

Generation of Ni-NCC complex: The NCC peptide was purchased from Genscript Corporation (Piscataway, NJ, USA). The Ni-NCC complex was generated using a transmetallation reaction performed in aqueous solution at neutral to basic pH. Incubation of the peptide for approximately 30 minutes with immobilized metal affinity chromatography (IMAC) resin (GE Healthcare) charged with nickel ensures a clean reaction with no undesired side products and no free metal ions in solution, yielding a reddish-brown complex.

ESI-MS: Samples were diluted 100x in methanol and analyzed on an LCT Premier (Waters Corporation) operating in negative ion mode (Figure S1). In order to verify that no changes were made to the peptide upon release of the metal, samples were acidified to approximately pH 5 by addition of 1 M hydrochloric acid (HCl) and analyzed using the same technique.

CD and absorption studies: A 1.5 mM solution of Ni-NCC was prepared in 50 mM sodium phosphate, pH 7.4, sparged with argon. Immediately after incubation, samples were placed in a cuvette with a 1 cm pathlength and scanned from 900-300 nm using both absorption and CD spectroscopy. Background scans of buffer alone were subtracted from each scan. Absorption studies were performed on an Agilent 8453 UV/Visible spectrophotometer. Circular dichroism analysis was performed on a J-815 (Jasco Corporation). The data presented are the average of five scans.

Deconvolution: Deconvolution of CD and absorption data was performed using Igor Pro (Wavemetrics). Iterative Gaussian deconvolutions were performed with a constant peak width of 1650 cm^{-1} . Absorption band energies were kept within 10% of the corresponding CD bands due to the broad nature of the absorption spectrum.

DFT: The *ORCA 2.7* software package designed by Neese and coworkers was used for all DFT computations.¹ Spin restricted geometry optimizations were converged to the $S = 0$ spin state and employed the Becke-Perdew (BP86) functional,^{2,3} and the aug-TZVP (Dunning diffuse functions added to Ahlrichs triple- ξ valence polarized) basis in conjunction with the TZV/J auxiliary basis for all atoms.^{4,5} These calculations employed the resolution of identity (RI) approximation developed by Neese.⁶ Solvation effects associated with water ($\epsilon = 80$) were incorporated using COSMO, as implemented in *ORCA*.⁷ Subsequent single-point energy calculations on the geometry-optimized structures employed the B3LYP functional,^{8,9} the aug-TZVP basis,¹⁰ and the COSMO solvation model.

pH titration: The absorption of the complex was monitored over a pH range of 7.4 to 10 to confirm that no structural changes result from pH adjustment. As observed with similar systems,¹¹ the peaks observed at pH 7.4 increase in intensity with increasing pH (Figure S2). To monitor the dependence of absorption intensity on pH, a sample containing 1.5 mM Ni-NCC was prepared in 50 mM borate at pH 10, sparged with argon. After incubation, the pH was adjusted back to 10 and the CD and absorption spectra were measured as described above. pH was lowered in half-log increments (pH 9.5, 9.0, 8.5, 8.0, and 7.4) using 1 M HCl, and CD and absorption spectra were collected at each pH point.

MCD: Samples containing 6 mM Ni-NCC were prepared in 50 mM borate at pH 10, sparged with argon. Solid sucrose was added as a glassing agent and the mixture was heated to form a saturated solution. The dilution resulted in a final Ni-NCC concentration of 2 mM. The sample was placed in an MCD cell and flash frozen. Spectra were collected on a J-815 (Jasco Corporation) interfaced with an Oxford Spectromag 4000. Spectra were collected at +7 and -7 Tesla and the difference was found via subtraction in order to remove any CD signal. Spectra were collected at 15 K, 8 K, 4.5 K, and 2 K and analyzed to identify any changes in the spectra that indicate paramagnetic character. The feasibility of correlating these low temperature data with the structure of Ni-NCC at room temperature is demonstrated by the lack of apparent changes in the corresponding CD spectra collected at 298 and 4.5 K (Figure S4). The only changes between these two spectra

are the expected blue-shifts and sharpening of the bands in the spectrum collected at 2 K. The percentage of paramagnetic species was determined by comparing the MCD intensity of the most intense feature in our spectrum to a purely paramagnetic tetrahedral Ni^{II} species (Ni^{II}-substituted Rubredoxin) at comparable field (5T) and temperature (4.5K) in $\Delta\epsilon$ ($M^{-1}cm^{-1}$). Qualitatively, our most intense feature occurs at 26 000 cm^{-1} with an intensity of $\sim 1 M^{-1}cm^{-1}$. In comparison, in the tetrahedral Ni^{II}-substituted Rubredoxin MCD spectrum, the most intense feature at 23 000 cm^{-1} has an intensity of $> 100 M^{-1}cm^{-1}$.¹² Therefore, under the assumption that the paramagnetic species observed for Ni-NCC has a similar $\Delta\epsilon$ value, this species represents approximately less than 1% of the overall sample.

Solid phase peptide synthesis: The peptides GCC, GGGCC, and GGNCC were synthesized in house using solid phase peptide synthesis on Wang resin using Fmoc protected amino acids and HBTU/DIPEA coupling techniques. Wang resin and Fmoc-protected amino acids were purchased from Novabiochem and used as received. The peptide was cleaved from the resin using Reagent R (90% TFA/5% thioanisole/3% EDT/2% anisole). The resulting solution was added dropwise to cold diethyl ether to precipitate the peptide. The cleavage solution was washed several times with cold ether and the resulting crude peptide was purified by preparative reverse phase HPLC (Shimadzu) with a C18 column (Varian Microsorb 300 C18; 8 μ M, 250 x 21.4) and guard column (Varian Microsorb 300 C18; 8 μ M, 50 x 21.4). The fractions containing the purified peptide were lyophilized and the mass was verified by ESI-MS.

Electrochemical studies: A 3 mL, 3 mM Ni-NCC sample was prepared in 50 mM borate at pH 10. CV data were collected with a CHI812C Electrochemical Analyzer potentiostat (CH Instruments) with a three-electrode setup (platinum working electrode, Bioanalytical Systems Inc.; Pt auxiliary electrode; Ag/AgCl reference electrode) in a glass CV cell. Potential was applied from zero to 1.2 V with a scan rate of 0.2 V per second, and current was measured (Figure S6). Bulk electrolysis was performed on a 3 mL, 3mM Ni-NCC sample prepared in the same manner. Using the same setup as the CV measurements, potential was applied at 0.95 V while stirring to fully oxidize the sample, and current was monitored until no further change was observed. ESI-MS operating in negative ion mode was performed on the sample following bulk electrolysis to confirm the peptide was unaltered.

Xanthine/xanthine oxidase SOD activity assay: An assay using xanthine/xanthine oxidase was performed as described by of Crapo *et al.*¹³ with minor modifications. The assay was performed in 50 mM potassium phosphate with 100 μ M EDTA at pH 7.8. 600 μ M cytochrome c from bovine heart (Sigma), 300 μ M xanthine (Sigma), and enough xanthine oxidase (from buttermilk; Sigma) to cause a change in absorbance at 550 nm of 0.02 to 0.04 per minute were added to a final volume of 300 μ L, and the change in absorbance at 550 nm was monitored on a Cary 100 UV-visible spectrophotometer (Varian). The assay was performed with several concentrations (0, 10, 15, 20, 25, 30, 35, 40, and 50 μ M) of Ni-NCC to measure an IC₅₀ value.

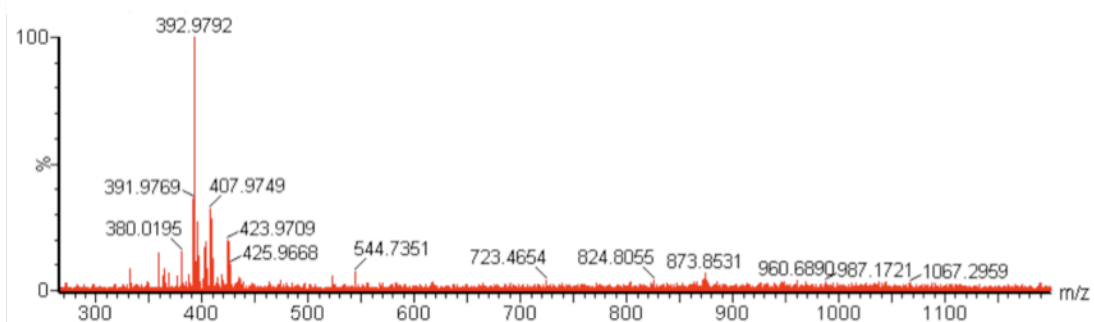


Figure S1. ESI-MS of Ni-NCC in 50 mM borate (pH 9.3 after incorporation of the metal). The major peaks correspond to the 1:1 Ni-NCC species. Additional peaks can be accounted for by considering nickel isotopes.

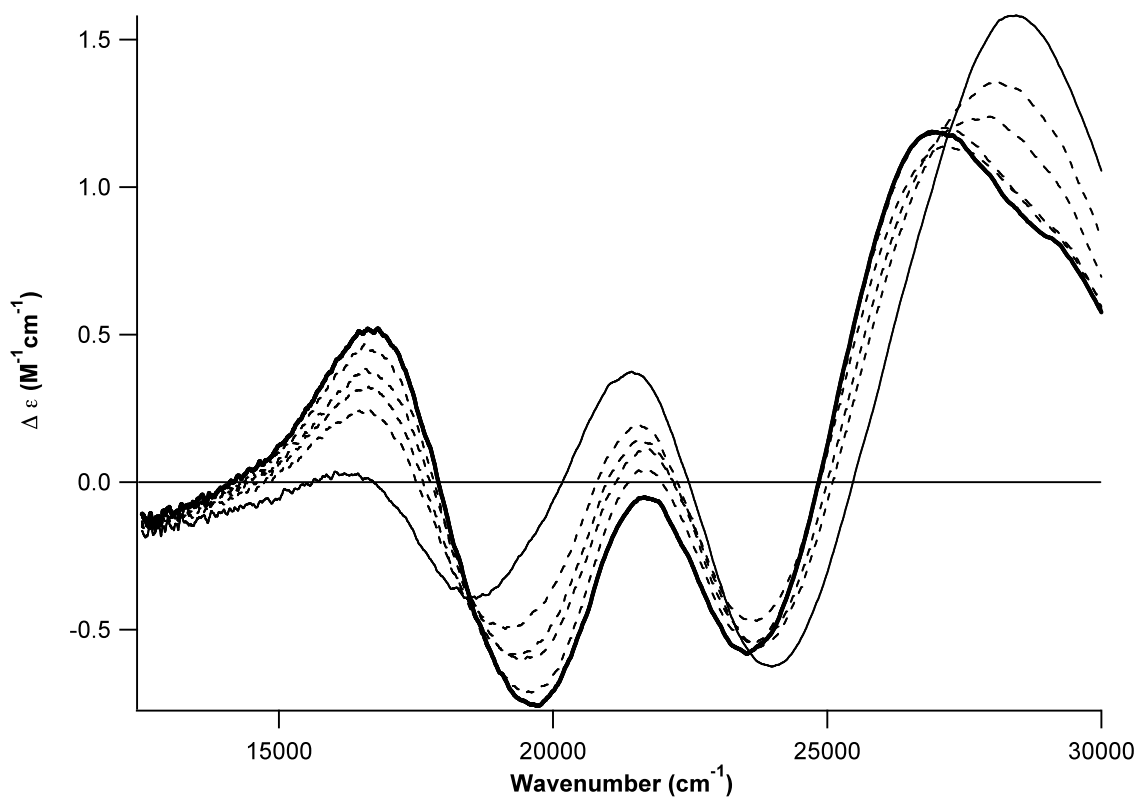


Figure S2. CD of a pH titration of Ni-NCC in 50 mM borate. The bold line represents the highest pH (10.0) and the solid line represents the lowest pH (7.4). Dashed lines represent other pH values measured (pH 9.5 – 8.0), in which the peaks are reduced in intensity with each half-log decrease in pH. The low energy bands corresponding to the d-d transitions are not as intense at lower pH.

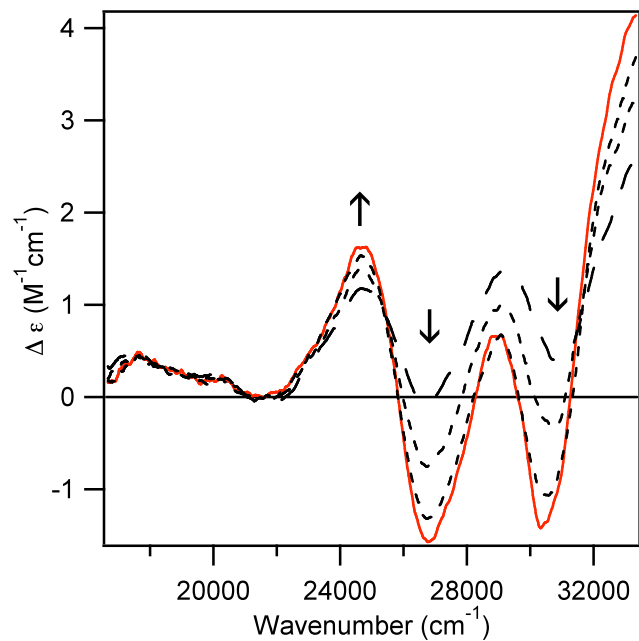


Figure S3. Variable temperature, 7 T MCD difference of Ni-NCC in a 34:66 solution of 50 mM borate:sucrose. Spectra show very little temperature dependence. (The solid red line represents data collected at 2 K, the dotted spectra were collected at 4.5 K and 8 K and the dashed line represents data collected at 15 K.)

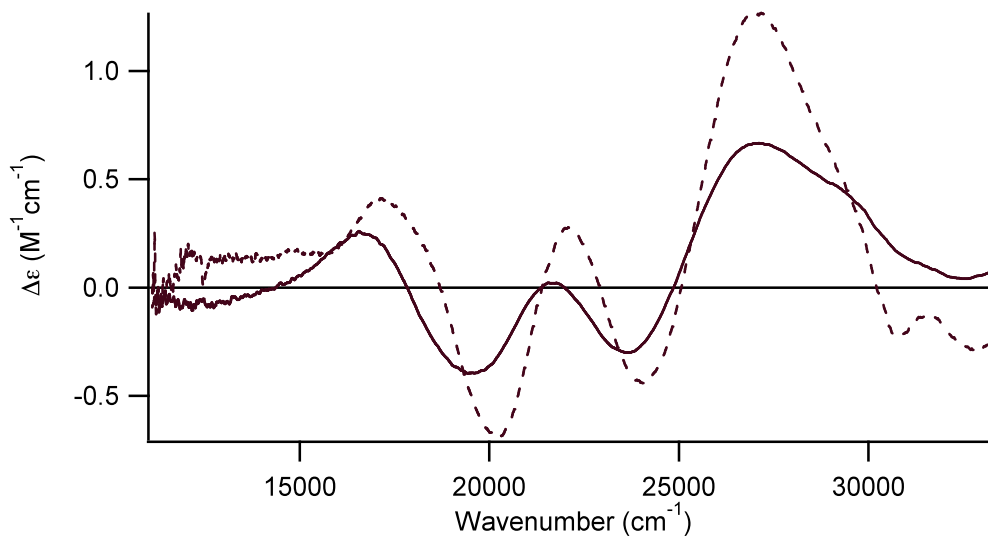


Figure S4. Room- and low-temperature CD spectra. The 4.5 K and 298 K spectra are represented as dashed and solid lines, respectively.

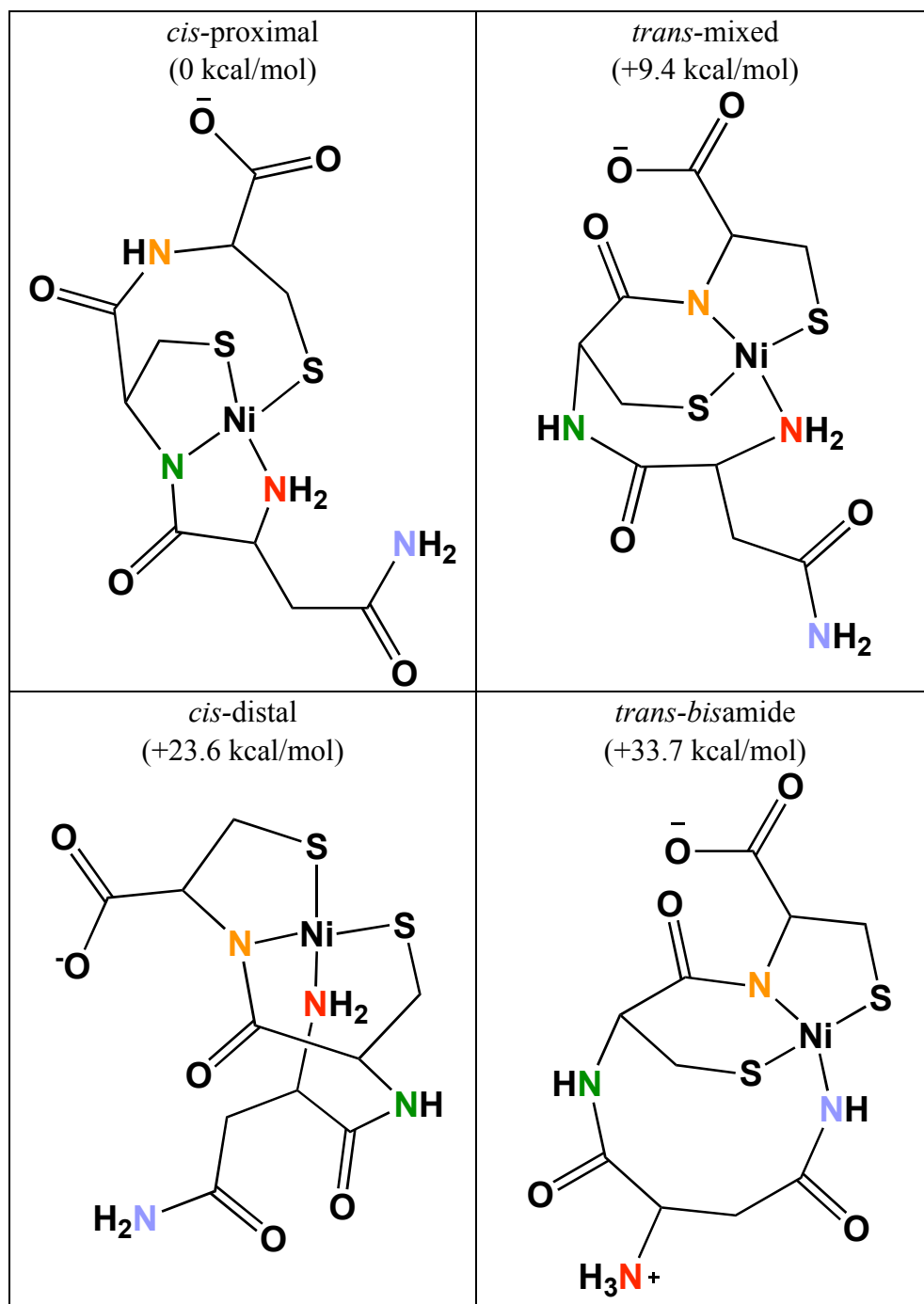


Figure S5. Energies of converged structures of Ni-NCC in various conformations. The lowest energy confirmation corresponds to Ni-NCC with *cis*-thiolates and the backbone amide and N-terminal amine nitrogens involved in coordination. Relative energies versus the lowest energy model (*cis*-proximal) are listed in kcal/mol. Nitrogen atoms are color coded to be consistent between models.

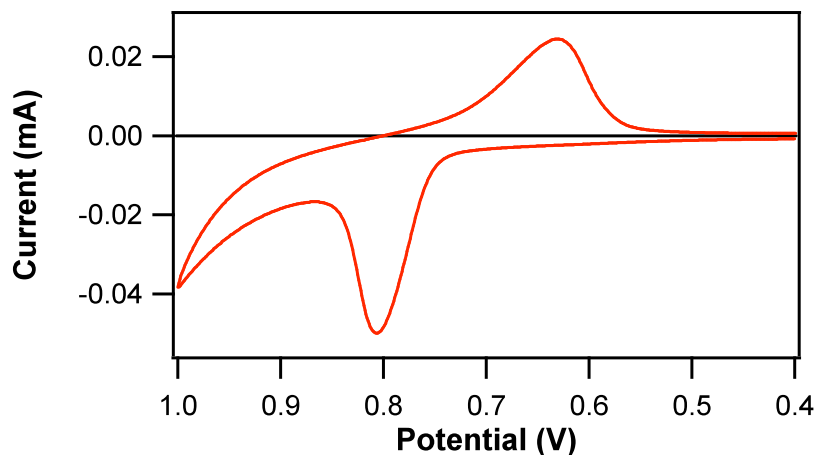


Figure S6. CV of Ni-NCC in 50 mM borate, pH 9.3, with a scan rate of 0.2 V per second. Electrochemically, the system is quasi-reversible ($E_m = 0.72(2)$ versus Ag/AgCl.)

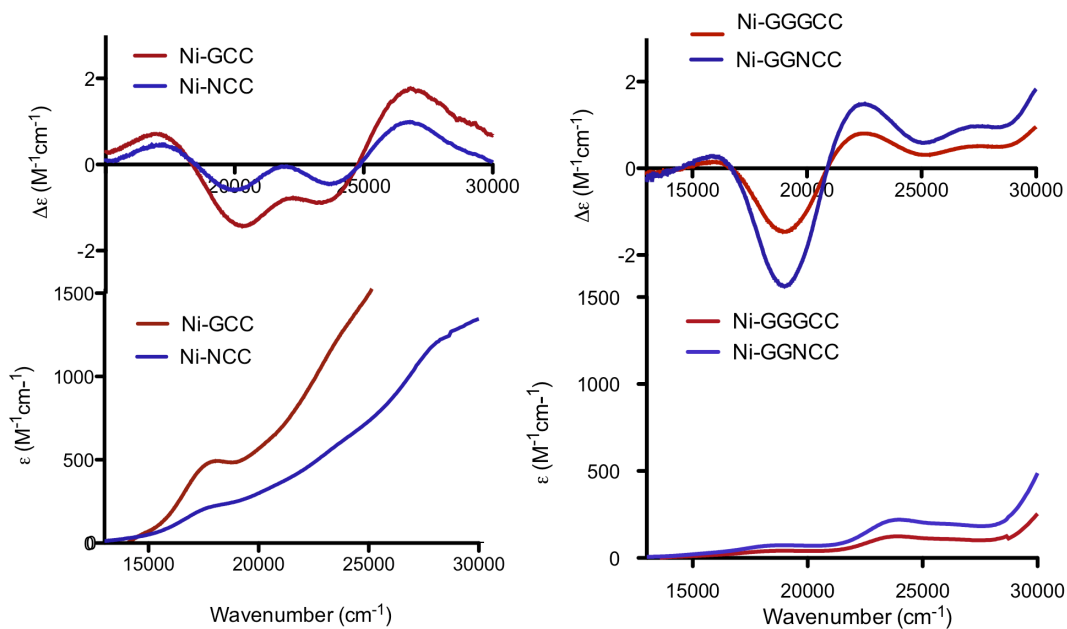


Figure S7. CD and absorption spectra of Ni-NCC, Ni-GCC, Ni-GGNCC, and Ni-GGGCC in 50 mM borate, pH 9.3. Differences in intensity reflect different abilities of the peptides to pick up metal, consequently altering concentrations of the overall metal-peptide species.

Table S1. Deconvolution of peaks in absorption and CD spectra of Ni-NCC.

	Absorption		CD	
	Energy (cm ⁻¹)	ϵ (M ⁻¹ cm ⁻¹)	Energy (cm ⁻¹)	$\Delta\epsilon$ (M ⁻¹ cm ⁻¹)
1	14 500	20	14 200	-0.1
2	17 300	60	16 270	-0.21
3	19 650	160	18 900	0.22
4	21 850	205	22 170	0.64
5	24 300	275	23 900	-0.44
6	26 850	575	26 520	0.71
7	28 850	1080	28 475	1.1

Supplemental References:

1. Neese, F. *ORCA – an ab initio, Density Functional and Semiempirical Program Package, Version 2.7*, University of Bonn, 2009.
2. Becke, A. D. *J. Chem. Phys.* **1986**, *84*, 4524-4529.
3. Perdew, J. P. *Physical Review B* **1986**, *33*, 8822-8824.
4. Schäfer, A.; Horn, H.; Ahlrichs, R. *J. Chem. Phys.* **1992**, *97*, 2571-2577.
5. Schäfer, G.; Huber, C.; Ahlrichs, R. *J. Chem. Phys.* **1994**, *100*, 5829-5835.
6. Neese, F. *J. Comput. Chem.* **2003**, *24*, 1740-1747.
7. Sinnecker, S.; Rajendran, A.; Klamt, A.; M., D.; Neese, F. *J. Phys. Chem. A* **2006**, *110*, 2235-2245.
8. Becke, A. D. *J. Chem. Phys.* **1993**, *98*, 5648-5652.
9. Becke, A. D. *J. Chem. Phys.* **1993**, *98*, 1372-1377.
10. Dunning, T. H., Jr. *J. Chem. Phys.* **1989**, *90*, 1007-1023.
11. Zoroddu, M. A.; Schinocca, L.; Kowalik-Jankowska, T.; Kozlowski, H.; Salnikow, K.; Costa, M. *Environ Health Perspect* **2002**, *110*, 719-723.
12. Kowal, A. T.; Zambrano, I. C.; Moura, I.; Moura, J. J. G.; LeGall, J.; Johnson, M. K. *Inorg. Chem.* **1987**, *27*, 1162-1166.
13. Crapo, J. D.; McCord, J. M.; Fridovich, I. *Methods Enzymol.* **1978**, *53*, 382-393.